

Electrochemical impedance measurements in non-stationary systems – application of the 4-dimensional analysis method for the impedance analysis of overoxidized poly(3,4-ethylenedioxythiophene)-modified electrodes

M. Ujvári¹, D. Zalka¹, S. Vesztergom¹, S. Eliseeva², V. Kondratiev², G. G. Láng^{1*}

¹ Institute of Chemistry, Laboratory of Electrochemistry and Electroanalytical Chemistry, Eötvös Loránd University, Pázmány P. s. 1/A, H-1117 Budapest, Hungary

² Chemical Department, St. Petersburg State University, Universitetskii pr. 26, 198504, Russia

Received March 10, 2017 Revised March 26, 2017

In this study it has been shown that the 4-dimensional analysis method, originally proposed by Stoynov, can not only be used for the correction of existing (experimentally measured) impedance data, but it also opens up the possibility of the estimation of impedance spectra outside the time interval of the measurements. As an illustrative example the method is applied for the determination of the charge transfer resistance of a polymer modified electrode corresponding to the time instant just after overoxidation of the poly(3,4-ethylenedioxythiophene) (PEDOT) film.

Key words: non - stationary system, instantaneous impedance, overoxidation of poly(3, 4 - ethylenedioxythiophene) (PEDOT), 3D complex interpolation method, charge transfer resistance..

INTRODUCTION

The single sine excitation method is by far the most commonly used technique for measuring impedance in electrochemical systems. In a single sine excitation measurement, the excitation signal is time-invariant and deterministic. When this method is employed the system under investigation is sequentially excited by applying small sinusoidal waves of a quantity, such as current or voltage. This is done within a given frequency range (e.g. from some mHz to some MHz). If the condition of linearity is fulfilled, the response of the system is an alternating voltage or current signal with the same frequency as that of the input signal. The frequency dependence of the response can be attributed to specific processes occurring either at the interfaces (electrodes) or inside the phases in contact. The impedance at a given frequency is the complex ratio of the Fourier transforms of the voltage and the current signals (sinusoids of the same frequency). A frequency spectrum can be obtained by sweeping the excitation frequency. Unfortunately single sine impedance spectroscopy measurements suffer from increasing time consumption if the frequency range is extended toward lower frequencies. When data recording occurs at low frequencies a complete measurement sequence can take significant time (at least several minutes).

However, many electrochemical systems are intrinsically nonstationary and are affected by time-dependent phenomena. According to the usual interpretation of the concept of impedance, impedance is not defined as time-dependent and, therefore, there should not exist impedance out of stationary conditions. On the other hand, it is possible to show that under some suitable conditions time dependence can be conciliated into the concept of impedance.

Stoynov pointed out that there are two general cases in the impedance measurements related to the non-stationary errors [1]:

(i) measurements in a stationary system under non-steady state conditions;

(ii) investigation of non-stationary systems.

The error of the first type increases sharply with decrease of the frequency (see ref. [2]). In the second case, an additional error appears, related to the measurement delay due to the classical “frequency by frequency” mode of impedance measurements.

Different methods to deal with a non-stationary behavior can be found in literature. Stoynov proposed a method of determining instantaneous impedance diagrams for non-stationary systems based on a four-dimensional approach [1, 3]. Darowicki et al. developed a dynamic EIS method to trace the dynamics of the degradation process by the calculation of an instantaneous impedance [4]. The possibility to analyze non-stationary impedance spectra by employing standard equivalent circuits was discussed in [5]. In [6] a procedure was proposed to quantify and correct

To whom all correspondence should be sent:
E-mail: langgyg@chem.elte.hu

for the time-evolution by means of the calculation of an instantaneous impedance. (The instantaneous impedance is defined as an instantaneous projection of the non-stationary state of the system into the frequency domain [1].)

The method of Stoynov (the 4-dimensional analysis) provides for correction of the systematic errors arising during the measurements of time-evolving impedance, i.e. when the consecutive impedance measurements are performed at different system states, but each of the measured impedance values can be accepted as “valid” in the classical sense. In this case the measured data are corrupted by typical errors caused by the system evolution during the experiment [7]. (If the problem is related to the mathematical basis of the transfer function analysis [2, 8], the so called rotating Fourier transform can be used [7, 9].)

As discussed before, the four-dimensional analysis method is based on the assumption for the continuum of the object’s state and parameters space. It requires a number of impedance spectra recorded subsequently at the same set of frequencies. Every measured data at a given frequency should additionally contain the time of measurement. Thus, the experimental data form a set of 4-dimensional arrays, containing frequency, real and imaginary components of the impedance and the time of measurement. The post-experimental analytical procedure previews the reconstruction of calculated instantaneous impedances. For every measured frequency two one dimensional functions of “iso-frequency dependencies” (e.g. for the real and for the imaginary components) are constructed. Then, each iso-frequency dependence is modeled by an approximating formal model. On the basis of the continuity of the evolution, interpolation (and extrapolation) is performed resulting in instantaneous projections of the full impedance-time space and “reconstructed” instantaneous impedances related to a selected instant of the time (i.e. the beginning of each frequency scan). Thus a set of impedance diagrams is obtained, containing instantaneous impedances, virtually measured simultaneously. Each of these diagrams can be regarded as a stationary one, free of non-steady-state errors.

On the basis of the above, one could conclude that the four-dimensional analysis method can be most effective in the correction of low-frequency impedance data. However, as it will be shown in the present study, this technique can also be used for solving other problems. For instance, it is known that the impedance spectra of overoxidized poly(3,4-ethylenedioxythiophene) (PEDOT) films

on gold recorded in aqueous sulphuric acid solutions differ from those measured for freshly prepared films. The most interesting feature is the appearance of an arc (or a “depressed semicircle”) at high frequencies in the complex plane impedance plot. The decreasing capacitance and the increasing charge transfer resistance suggest that during overoxidation the electrochemical activity of the film decreases and the charge transfer process at the metal/film interface becomes more hindered than in the case of pristine films. The published results support the mechanistic picture, according to which the originally compact and strongly adherent polymer films undergo structural changes during the overoxidation (degradation) process [10-16]. Overoxidation results in the partial delamination of the polymer layer and leads to the exposure of some parts of the underlying metal substrate to the electrolyte solution.

Nevertheless, it should be emphasized here that the polymer film still present on the substrate after overoxidation remains electroactive, and its internal structure may be an interesting subject for further studies, since according to literature reports conducting polymers in different overoxidation states show unique features useful for analytical, sensing and biomedical applications [17-22].

The time evolution of the impedance spectra is a remarkable feature of the electrodes with overoxidized PEDOT films. To our knowledge, this phenomenon was first reported in ref. [23]. According to this observation, the charge transfer resistance at the (electronically conductive) substrate/polymer film interface decreases continuously over several hours when the potential is held in the “stability region” after overoxidation of the film. This means that the impedance spectra recorded using the consecutive frequency sweep mode (typical of EIS) are corrupted by typical errors caused by the system evolution during the experiment. On the other hand, for reasons of measuring technology, we are not able to record an impedance spectrum immediately after the overoxidation process. But even if we would be able to do so it wouldn’t solve the problems related to the nonstationarity of the system. It is beyond doubt that the knowledge of the “initial” charge transfer resistance is essential for the better understanding of the degradation process and it may also have an impact on practical applications.

In the present study, an attempt was made to solve both problems simultaneously by using a method very similar to that proposed by Stoynov.

EXPERIMENTAL

Electrodeposition of PEDOT

Poly(3,4-ethylenedioxythiophene) films were prepared by galvanostatic deposition on both sides of thin gold plates from 0.01 mol·dm⁻³ ethylenedioxythiophene (EDOT) solution containing 0.1 mol·dm⁻³ Na₂SO₄ supporting electrolyte. Analytical grade 3,4-ethylenedioxythiophene (Aldrich), p.a. Na₂SO₄ (Fluka), and ultra-pure water (specific resistance 18.3 MΩ·cm) were used for solution preparation. All solutions were purged with oxygen-free argon (Linde 5.0) before use and an inert gas blanket was maintained throughout the experiments.

The deposition was performed in a standard three electrode cell in which the gold plate in contact with the solution served as the working electrode (WE). A spiral shaped gold wire immersed in the same solution served as the counter electrode (CE), and a KCl-saturated calomel electrode (SCE), as the reference electrode (RE). A constant current density of $j = 0.2 \text{ mA}\cdot\text{cm}^{-2}$ ($I = 0.2 \text{ mA}$) was applied for 1000 s (the geometric surface area of the working electrode was 1 cm²). The film thickness was estimated from the polymerization charge by using the charge/film volume ratio determined earlier by direct thickness measurements [24-26]. The average thickness of the PEDOT film was about 0.8 μm, the structure of the PEDOT film was globular, cauliflower-like.

Cyclic voltammetry and impedance measurements

Solutions used for cyclic voltammetric and impedance measurements were prepared with ultra-pure water and p.a. H₂SO₄ (Merck). The solutions were purged with oxygen-free argon (Linde 5.0) before use and an inert gas blanket was maintained throughout the experiments. In the conventional three-electrode cell configuration the PEDOT-modified gold substrate in contact with the solution was used as the working electrode (WE), a spiral shaped gold wire immersed in the same solution as the counter electrode (CE), and a NaCl-saturated calomel electrode (SSCE) as the reference electrode (RE). The counter electrode was arranged cylindrically around the working electrode to maintain a uniform electric field.

The overoxidation of the PEDOT film was carried out in 0.1 mol·dm⁻³ H₂SO₄ solution a day after the deposition.

A Zahner IM6 electrochemical workstation was used in all electrochemical experiments.

RESULTS AND DISCUSSION

Cyclic voltammetry and overoxidation of the PEDOT-film

The potential program applied to the PEDOT-modified electrode used in the impedance measurements (geometric surface area: 1.0 cm²) is given in Fig.1a, and the corresponding cyclic voltammograms in Fig.1b. The cyclic voltammograms recorded before and after overoxidation of the gold|PEDOT|0.1 mol·dm⁻³ sulfuric acid (aq.) electrodes were very similar to those reported in the literature (see e.g. [13, 27]).

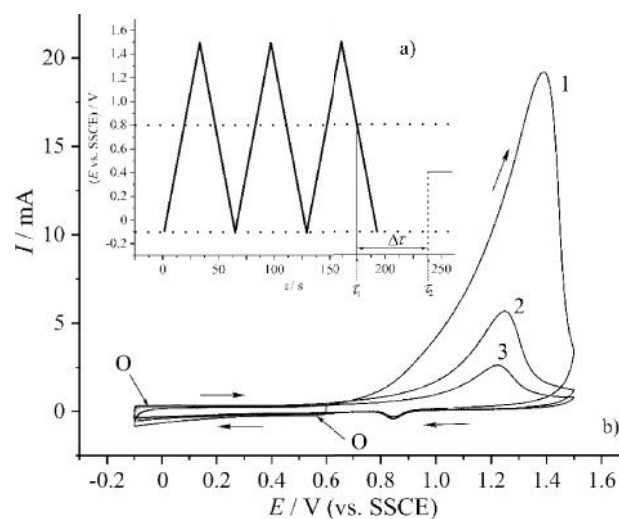


Fig. 1. a) The potential program applied to the PEDOT-modified electrode. The impedance measurements started at t_1 is the estimated end of the overoxidation process. $t_2 = 66.4 \text{ s}$. b) O: Cyclic voltammogram recorded before overoxidation in the potential range between - 0.1 V and 0.6 V vs. SSCE, sweep rate: $v=50 \text{ mV/s}$. 1-3: Successive cyclic voltammograms („overoxidation cycles”) recorded in the potential range from - 0.1 V to 1.50 V vs. SSCE, sweep rate: $v=50 \text{ mV/s}$.

In the 3 overoxidation cycles, the positive potential limit has been set to 1.5 V vs. SSCE (Fig. 1a). It is known [11-15] that between - 0.3 and 0.8 V vs. SSCE the oxidation-reduction process of the PEDOT films is reversible. However, at more positive potentials irreversible degradation of the polymer layer occurs. As it can be seen in Fig. 1b (curve O), the cyclic voltammograms of PEDOT-modified electrodes show almost pure capacitive behavior in the potential range between -0.1 V and +0.6 V, i.e. if the positive potential limit is kept below 0.8 V vs. SSCE. If the polarization potential exceeds this critical value, an oxidation peak without corresponding reduction peak appears (see Fig. 1b). The voltammograms recorded before

and after overoxidation are similar in shape and show typical (pseudo-)capacitive behavior, but the redox capacity of the (over)oxidized polymer film is considerably smaller than that of the freshly prepared film.

Impedance measurements

After overoxidation, subsequent impedance measurements were performed at 0.4 V vs. SSCE over a frequency range from 100 mHz to 100 kHz (starting at t_2 in Fig. 1a).

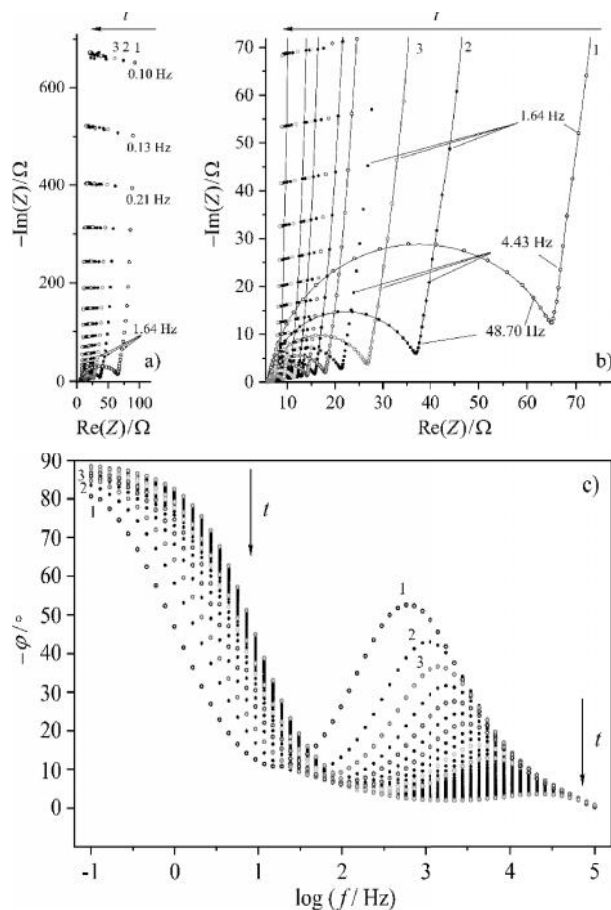


Fig. 2. a) Successive impedance diagrams of the Au | PEDOT | 0.1 M H₂SO₄ at $E = 0.4$ V vs. SSCE recorded after overoxidation; b) High frequency part of the Argand diagrams; c) Phase angles corresponding to a); The solid lines are to guide the eye only: not curve fits.

The data points were measured at 60 discrete frequencies in the frequency region investigated during each scan at an amplitude of 5 mV.

In Fig. 2 the results are presented in the complex plane. The 3D representation of the data is shown in Fig. 3. The curves in Figs. 2 and 3 are similar to those reported for other polymer modified electrodes [28, 29], all the complex plane diagrams contain a capacitive semicircle and a Warburg-like region (quite narrow) followed by a CPE-like domain at low frequencies

[30]. However, since the successive impedance diagrams are continuously changing with time (see Figs. 2 and 3), it is obvious that the system is still in a transient state rather than in a stationary (or equilibrium) state.

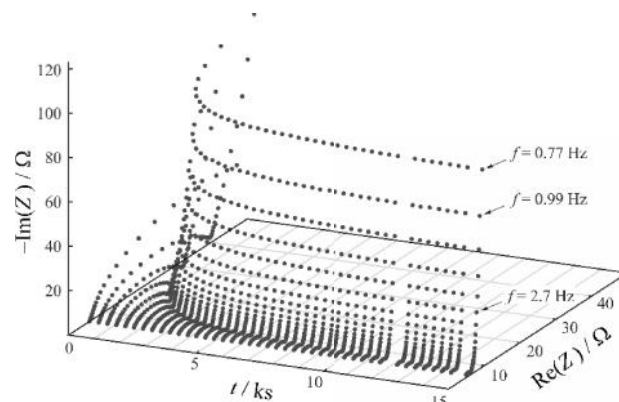


Fig. 3. Time dependence of the locus curves of recorded impedance spectra in the Argand-representation.

As already discussed in the introduction, in such cases a post-experimental analytical procedure is necessary for the reconstruction of “instantaneous impedances” [2, 3, 7, 9, 31-33].

For this purpose a 3D complex interpolation method using a three-dimensional bicubic spline interpolation algorithm implemented in LabVIEW [34] has been adopted. Mathematically, this corresponds to the 4-dimensional analysis proposed by Stoynov [1-3, 7].

Two different approaches were applied for the calculation of the corrected (synthetic) impedance diagrams. In the first, the measured magnitudes and phase angles were used in the interpolation/extrapolation process (Fig. 4), and the interpolated/extrapolated magnitude and phase angle values corresponding to the same time moments were converted into real and imaginary parts of the complex impedance. In the second, the interpolation/extrapolation was carried out using real and imaginary parts of impedances measured at identical frequencies („isofrequential components”) [1] (see Fig. 5). This means that for every measured frequency two one-dimensional functions of iso-frequency dependencies (for the real and for the imaginary components) have been constructed, and on the basis of the continuity of the evolution, interpolation (and extrapolation) has been performed. As a result a set of instantaneous impedances related to a selected instant of time (i.e. the beginning of each frequency scan) has been obtained.) As it can be seen by comparing Figs 4 and 5, the corrected impedances obtained by the two methods practically coincide.

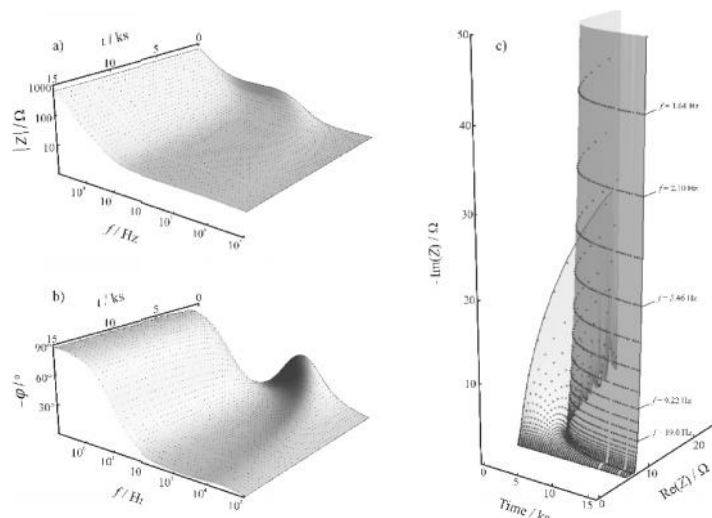


Fig. 4. Results of a 3D complex interpolation. The absolute values (a) and phase angles (b) of measured impedances are shown as a function of time and frequency (discrete points). The continuous surface is created by a three-dimensional bicubic spline interpolation algorithm implemented in LabVIEW [1]. In (c) both the measured data (discrete points) and the interpolated surface are transformed to a time-dependent complex plane representation.

According to the above considerations, extrapolation allows the reconstruction of spectra that can be regarded as “original” (undistorted) from a series of time-dependent spectra. By extrapolation to $t = 0$ (2 in Fig. 1) the impedance diagram corresponding to the starting time of the measurement series could be constructed (Fig. 6, plots designated by S2)

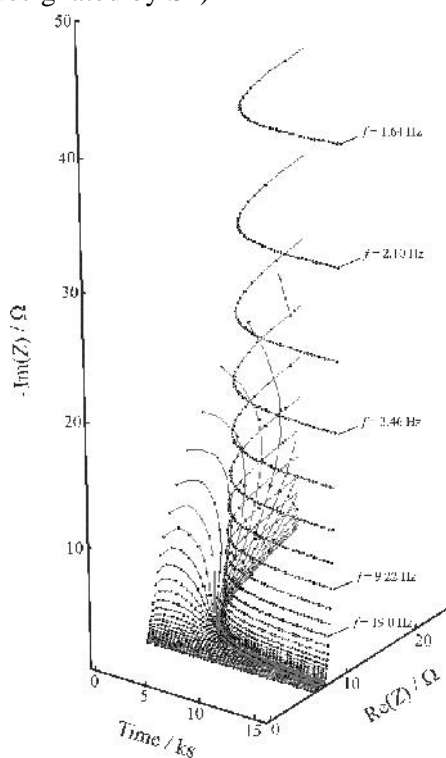


Fig. 5. The measured impedance spectra and some isofrequent space curves created by spline interpolation shown in a three-dimensional (time dependent) complex plane representation.

The differences between the diagrams S1 (directly measured data points) and S2 (calculated values for $t = 0$ s) in Fig. 6 are assumed to a first approximation to be entirely due to time evolution of the charge transfer resistance (R_{ct}) at the gold substrate/polymer interface. The value of the charge transfer resistance at $t = 0$ s was estimated by fitting the high-frequency impedance data (frequency range 38.57 Hz – 10.65 kHz) to an equivalent-circuit analog, shown in the inset of Fig. 7. The equivalent-circuit analog is based on the impedance model proposed in [29], wherein the double layer capacitance at the substrate/polymer interface has been replaced by a constant-phase element (CPE), which more accurately imitates the behavior of the double layer ($Z_{CPE} = \frac{1}{B}(i)^{-a}$, where i is the imaginary unit, B and a are the CPE parameters, and ω is the angular frequency, respectively).

The estimated values of the parameters (obtained by complex non-linear least squares (CNLS) fitting based on the Levenberg–Marquardt algorithm [35, 36]) are shown in the first column of Table. 1. Curve F1 in Fig. 7 is the complex plane diagram (Argand plot) simulated by using these parameters.

All the above results imply that the extrapolation method can not only be used for the correction of experimental data (i.e. the measured impedances), but it opens up the possibility of the estimation of the impedance spectra outside the time interval of the impedance measurements.

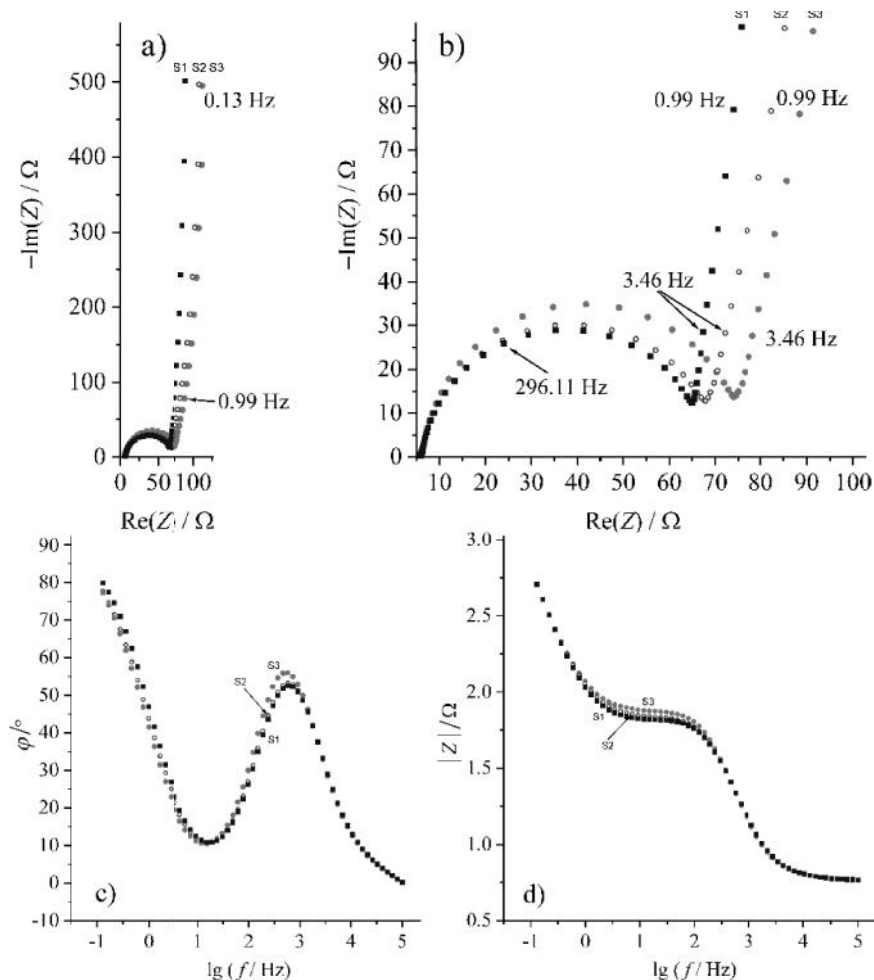


Fig. 6. S1 (■): Data measured during the frequency sweep starting at t_2 in Fig. 1. $t = 0$ is the starting time of the impedance measurement series. S1 is the first set of data measured in the series and contains inherent time dependence; S2 (○): corrected impedance diagram obtained by extrapolation to $t = 0$ (the „instantaneous” spectrum corresponding to the starting time of the impedance measurement series); S3 (□): calculated spectrum corresponding to the presumed end of the overoxidation process, $t = -66.4$ s (t_1 in Fig. 1). The data are shown in complex plane (a,b) and in Bode (b,c) representations.

Complex plane and Bode plots of the calculated impedance corresponding to the presumed end of the overoxidation process are shown in Fig. 6 (plots marked by S3). Similarly to the charge transfer resistance at $t = 0$ s, the R_{ct} at $t = -66.4$ s was obtained by CNLS fitting of the extrapolated data (frequency range 38.57 Hz – 10.65 kHz) [29, 36,37]. The best-fit values of the parameters are shown in the 2nd column of Table. 1, while F2 in Fig. 7 is the impedance spectrum calculated by using the estimated parameters.

As it can be seen from Fig. 7, the model function fits the extrapolated impedance data for $t = 0$ s quite well, for $t = -66.4$ s the goodness of the fit is poorer. This is most probably the consequence of the very rapid time evolution of the impedance response immediately after overoxidation of the PEDOT film.

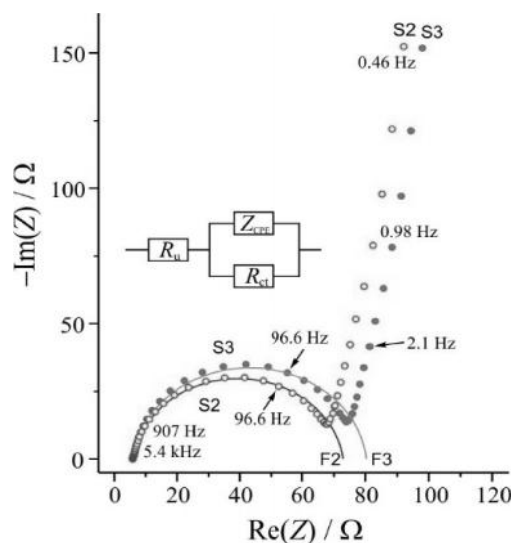


Fig. 7. S2 and S3: Impedance diagrams containing the „instantaneous impedances”, virtually measured simultaneously at $t = 0$ s (S2) and at $t = -66.4$ s (S3). F2 and F3: Impedance spectra calculated by using the estimated („best-fit”) parameters.

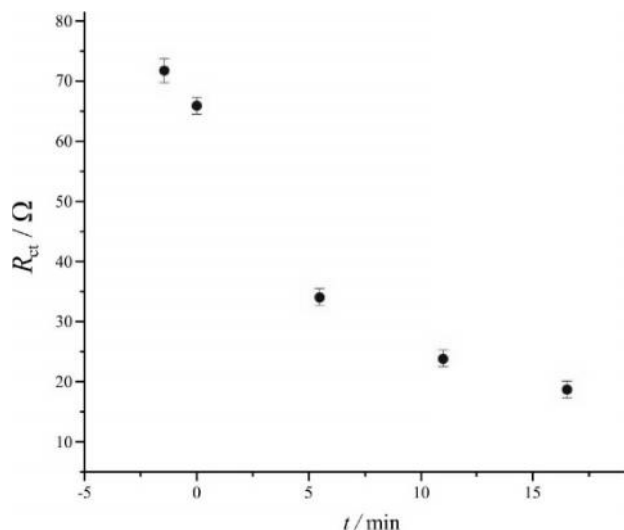


Fig. 8. Time evolution of the charge transfer resistance at the beginning of the experiment. The R_{ct} values are determined from the calculated impedance spectra.

Table 1. EDS surface composition of BCY15 and BCY15/Ni.

	$t = 0$ s	$t = -66,4$ s
	Estimated mean values with confidence intervals at 95% confidence level	Estimated mean values with confidence intervals at 95% confidence level
R_u/Ω	5.97 ± 0.27	5.97 ± 0.41
R_{ct}/Ω	67.0 ± 1.1	74.4 ± 1.6
B/Fs^{a-1}	$(1.064 \pm 0.063) \cdot 10^{-5}$	$(1.141 \pm 0.093) \cdot 10^{-5}$
a	0.925 ± 0.012	0.939 ± 0.017

Some of the charge transfer resistance values determined by using the “instantaneous” impedances are shown in Fig. 8. It can be seen from Table 1 (and from Fig. 8), that the highest value of R_{ct} is about 75 Ω . This value corresponds to the time instant just after overoxidation of the film. Starting from this value, R_{ct} decreases continuously with experimental time to a value somewhat higher than the charge transfer resistance of the pristine electrode.

CONCLUSIONS

The 4-dimensional analysis method, originally proposed by Stoynev, can serve as an efficient tool for the study of non-stationary systems. It can not only be used for the correction of the existing (experimentally measured) impedance data, but it opens up the possibility for the estimation of the impedance spectra outside the time interval of the

impedance measurements. The method was successfully applied for the determination of the charge transfer resistance of a gold|PEDOT|0.1 mol·dm⁻³ sulfuric acid (aq.) electrode corresponding to the time instant just after overoxidation of the PEDOT film. In the experiment presented in this study, the “starting” (calculated) R_{ct} value was approximately 75 Ω ·cm². After 66.4 seconds this value fell to about 67 Ω ·cm², i.e. it decreased by ~10 % in the first minute after the overoxidation procedure.

On the other hand, we acknowledge that criticism may arise from the choice of the method used to overoxidize the polymer film before the impedance measurements, since between the end of the last CV and the start of the first impedance measurement (t_2 in Fig. 1a) the electrode was held at the open circuit potential. Nevertheless the extrapolation procedure may be justified by the fact that according to experimental observations the impedance parameters of the Au|PEDOT|0.1 mol·dm⁻³ sulfuric acid (aq.) electrode are practically independent of the electrode potential within a wide potential range (here between -0.1 and -0.8 V vs. SSCE). It should also be noted that in most practical cases no or only little information is available about the past history of the system involved. Therefore, because the measured data are from a time series experiment carried out within a given time period, any extrapolation beyond this time period is somewhat arbitrary.

Acknowledgements: Financial support from the Hungarian Scientific Research Fund (grants No. K 109036) and from the Russian Foundation for Basic Research (grant N-16-03-00457) are gratefully acknowledged.

REFERENCES

1. Z. Stoynev, B. Savova-Stoynev, *J. Electroanal. Chem.*, **183**, 133 (1985).
2. Z. Stoynev, B. Savova, *J. Electroanal. Chem.*, **112**, 157 (1980).
3. B. Savova-Stoynev, Z. Stoynev, *Electrochim. Acta*, **37**, 2353 (1992).
4. K. Darowicki, *J. Electroanal. Chem.* **486**, 101 (2000).
5. A. Battistel, G. Du, F. La Mantia, *Electroanalysis*, **28**, 2346 (2016).
6. T. Breugelmans, J. Lataire, Th. Muselle, E. Tourwé, R. Pintelon, A. Hubin, *Electrochim. Acta*, **76**, 375 (2012).
7. Z. Stoynev, *Electrochim. Acta*, **38**, 1919 (1993).
8. M. Keddou, Chr. Rakotomavo, H. Takenouti, *J. Appl. Electrochem.*, **14**, 437 (1984).
9. Z. Stoynev, *Electrochim. Acta*, **37**, 2357 (1992).

10. A. Zykwincka, W. Domagala, B. Pilawa, M. Lapkowski, *Electrochim. Acta*, **50**, 1625 (2005).
11. M. Ujvári, M. Takács, S. Vesztergom, F. Bazsó, F. Ujhelyi, G.G. Láng, *J. Solid. State. Electrochem.*, **15**, 2341 (2011).
12. G. Láng, M. Ujvári, F. Bazsó, S. Vesztergom, F. Ujhelyi, *Electrochim. Acta*, **73**, 59 (2012).
13. M. Ujvári, J. Gubicza, V. Kondratiev, K.J. Szekeres, G.G. Láng, *J. Solid. State. Electrochem.*, **19**, 1247 (2015).
14. M. Ujvári, G.G. Láng, S. Vesztergom, K.J. Szekeres, N. Kovács, J. Gubicza, *J. Electrochem. Sci. Eng.*, **6**, 77 (2015).
15. G. Láng, M. Ujvári, S. Vesztergom, V. Kondratiev, J. Gubicza, K. Szekeres, *Z. Phys. Chem.*, **230**, 1281 (2016).
16. G. Láng, C. Barbero, Laser techniques for the study of electrode processes, in: Monographs in electrochemistry, F. Scholz (Ed.), Springer, Berlin Heidelberg, 2012.
17. N. Kovács, M. Ujvári, G.G. Láng, P. Broekmann, S. Vesztergom, *Instrum. Sci. Technol.* **43**, 633 (2015).
18. J. Li, X-Q. Lin, *Sens. Actuators B*, **124**, 486 (2007).
19. D.C. Martin, J. Wu, C.M. Shaw, Z. King, S. Spanninga, S. Richardson-Burns, *J. Hendricks, J. Yang, Polym. Rev.* **50**, 340 (2010).
20. Z. Zhuang, J. Li, R. Xu, D. Xiao, *Int. J. Electrochem. Sci.*, **6**, 2149 (2011).
21. Y. Hui, C. Bian, J. Wang, J. Tong, S. Xia, *Sensors*, **17**, 628 (2017).
22. M. Irimia-Vladu, *Chem. Soc. Rev.*, **43**, 588 (2014).
23. G.G. Láng, M. Ujvári, Z. Dankházi, S. Vesztergom, K.J. Szekeres: Analysis of impedance spectra of electrochemically deposited PEDOT films recorded before and after overoxidation, 10th International Symposium on Electrochemical Impedance Spectroscopy, A Toxa, Spain, June 19 - 24, 2016, Book of Abstracts, p.16 (0720).
24. J. Bobacka, A. Lewenstam, A. Ivaska, *J. Electroanal. Chem.*, **17**, 489 (2000).
25. A. Stoyanova, V. Tsakova, *J. Solid State Electrochem.* **14**, 1947 (2010).
26. W. Poppendieck, K.P. Hoffmann, in: J. Vander Sloten, P. Verdonck, M. Nyssen, J. Haueisen (Eds.), ECIFMBE 2008, IFCMBE Proceedings 22, Springer-Verlag, Berlin, Heidelberg, 2009, p. 2409.
27. D. Zalka, N. Kovács, K. Szekeres, M. Ujvári, S. Vesztergom, S. Eliseeva, V. Kondratiev, G.G. Láng, *Electrochim. Acta*, submitted.
28. G. Inzelt, G. Láng, *Electrochim. Acta*, **36**, 1355 (1991).
29. G. Inzelt, G. G. Láng, Electrochemical Impedance Spectroscopy (EIS) for Polymer Characterization, Ch. 3, in: Electropolymerization: Concepts, Materials and Applications, S. Cosnier, A. Karyakin (Eds.), Wiley-VCH Verlag GmbH & Co. KGaA, Weinheim, 2010.
30. G. Láng, K.E. Heusler, *J. Electroanal. Chem.*, **481**, 227 (2000).
31. Z. Stoynov, in Materials for Lithium-Ion Batteries 1999, C. Julien and Z Stoynov, Eds, 85, p. 359, NATO Science Series, Kluwer Academic Publishers, Dordrecht, Boston, London, 2000.
32. Z. Stoynov, B. Savova-Stoynov, T. Kossev, *J. Power Sources*, **30**, 275 (1990).
33. B. Savova-Stoynov, Z. Stoynov, *Key Eng. Mater.*, **59-60**, 273 (1991).
34. W.H. Press, S.A. Teukolsky, W.T. Vetterling, B.P. Flannery (Eds) *Numerical Recipes in C++: The Art of Scientific Computing*. 2nd ed. Cambridge: Cambridge University Press, 2002.
35. D. Marquardt, *SIAM J. Appl. Math.*, **11**, 431 (1963).
36. P. Valkó, S. Vajda, Advanced scientific computing in BASIC with applications in chemistry, biology and pharmacology, Data handling in science and technology, Vol. 4, Elsevier, Amsterdam, 1989.
37. G. Inzelt, G. Láng, *J. Electroanal. Chem.*, **378**, 39 (1994).

4-D
 (3,4-)-
 1, 1, 1, 2, 2, 1
 1, , , . . 1 / , -1117 ,
 2, " , " , 26, 198504,
 10 2017 .; 26 2017 .
 ()
 4- , ,
 () ,
 ethylen) (PEDOT) . (3,4-